Journal of Operation and Automation in Power Engineering
Vol. 5, No. 2, Dec. 2017, Pages: 105-116
http:// joape.uma.ac.ir

A New Control Method for Single-Phase Grid-Connected Inverter Using Instantaneous Power Theory

M. Heidari [1], *M.A. Shamsi-Nejad* [*,1], *M. Monfared* [2]

[1] *Faculty of Electrical and Computer Engineering, University of Birjand, Birjand, Iran.*
[2] *Ferdowsi University of Mashhad, Mashhad, 91779-48974, Iran.*

Abstract- *Because of installation for local consumers and since it is free of all contaminations, connecting photovoltaic cells to the grid via single-phase inverter is significantly on the rise. In this paper, a new simple current control is proposed for single-phase grid connected voltage source inverter. Using the pq theory and modeling a single-phase system as an unbalanced three-phase system, a method is provided for reference current generation. In the proposed method, it is not necessary to generate a fictitious phase for the current signal. Also, the removal of adjusting filter parameters which were used to generate fictitious current signal increases the simplicity of the control system and reduces computational efforts, especially in the presence of distortion in current. The simulation results confirm that the proposed method provides a precise and fast current control with minimum harmonic distortions.*

Keyword: Grid-tie inverter, Modified instantaneous power theory, Reference current generation. precise

1. INTRODUCTION

The advancement in technology, problems caused by establishing and maintaining big powerhouses, and heavy losses of global transmission and distribution networks have led to an increase in using Distributed Generation (DG) resources in power systems and made these generators a new strategy for electricity companies in supplying electrical energy. On the other hand, as a result of the growing demand for energy worldwide and diminishing fossil of fuels, it is necessary to define new alternative energy sources to cover all future energy demands. In the past years, the application of renewable energies, particularly wind and solar energies, has been rising increasingly.

Within the past 20 years, solar electrical energy has had a 30% growth. As can be seen in Fig. 1, the installation of photovoltaic systems in 2015 broke the record in the world and reached 0.9 GW [1]. Meanwhile, the grid-connected PV has the largest contribution in the market. One of the most important parts of PV modules is grid connected inverters.

In the meantime, the connection of photovoltaic panels to the network through single-phase inverters has particularly increased due to their advantages, ease of installation for local consumers, and being free from all types of pollution. Voltage source inverters are widely applied for connection to the grid [2-3]. The topology of these inverters can be classified into two groups: single-stage and two-stage inverters. Single-stage inverters have two responsibilities: augmenting the input voltage and generating sine wave or one-sided sinusoidal wave.

As it is evident in Fig. 2, in the two-stage topology, the first step is used for boosting or reducing the DC input voltage as much as it becomes adapted to network voltage and then converting it to AC. Despite the low efficiency difference in two-step topologies, they are widely used due to the higher -

Received: 27 July 2016
Revised: 20 Sept. 2016 and 29 Nov. 2016
Accepted: 16 Dec. 2016
∗Corresponding author:
E-mail: mshamsi@birjand.ac.ir (M. A. Shamsi-Nejad)
Digital object identifier: 10.22098/joape.2017.2592.1225

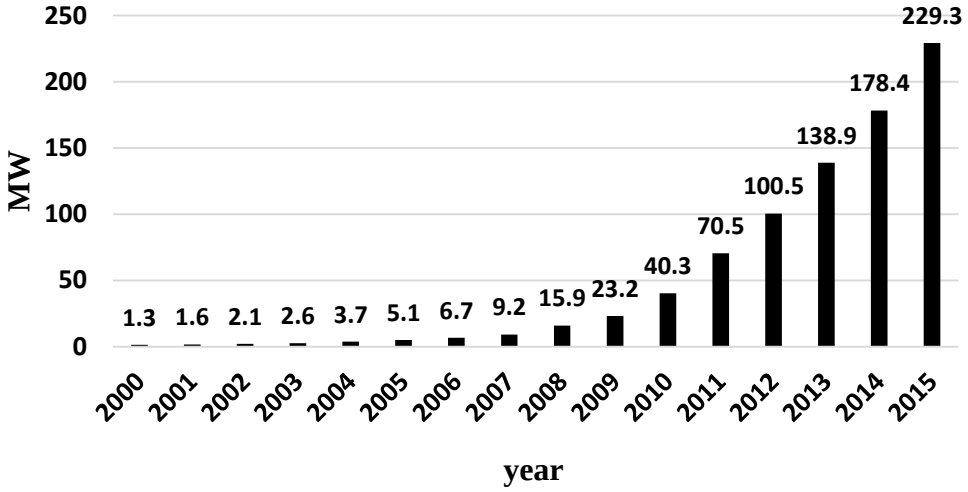

Fig. 1. Global cumulative capacity of PV systems installed in recent years [1]

- stability of DC voltage and network side voltage and lower harmonics [4-7].

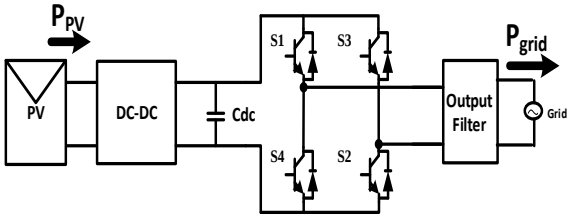

Fig. 2. Two-stage grid-tie single phase inverter

Considering voltage and sinusoidal current, the injection of power to the grid in a single-phase system is as follows:

$$P_{grid}(t) = V_{grid}(t) I_{grid}(t) \quad (1)$$

$$\begin{cases} V_{grid}(t) = V_m \cos(\omega t) \\ I_{grid}(t) = I_m \cos(\omega t - \varphi) \end{cases} \quad (2)$$

Where V_m and I_m are the amplitudes of the grid voltage and current. ω is grid frequency and ϕ is phase difference between voltage and gird current. Placing Equation (2) in (1) results in:

$$P_{grid}(t) = \frac{V_m I_m}{2} \cos(\varphi) + \frac{V_m I_m}{2} \cos(2\omega t - \varphi) \quad (3)$$

When the power factor is unit, this equation can be rewritten as.

$$P_{grid}(t) = P_{PV} + P_{PV} \cos(2\omega t) \quad (4)$$

As shown in Eq. (4), the instantaneous power injected to the network is comprised of two terms: the average output power, and the varying terms that oscillates at twice the grid frequency.

The task of the control system is to maintain the balance of power (similar to Eq. (4)) by controlling the power extracted from photovoltaic panels and power injected into the grid. It is worth mentioning that power oscillates at twice the grid frequency which is usually provided by DC link capacitors.

There have been various methods to control inverter current in order to transfer this power and reduce network-injected current harmonic. In these methods, by generating the appropriate inverter switching state, the signal error is eliminated due to the difference between the reference value and the measured current. It should be noted that L-type smoothing filters such as LC or LCL are usually used for inverter output current. In addition, the proper performance of the inverter mostly depends on the quality of the reference currents generation and the switching states. Hysteresis band current control [8-12], synchronous reference frame-based method [13-17], and controlling based on proportional resonance controller (PR) [2, 18-22] are common generations of reference currents for controlling the switches. The hysteresis current control method is a simple method creating a fixed band over the reference current to control the inverter output current. Because the output of hysteresis controller is in the form of signals used for gate triggering, there is no need for PWM block to generate pulses that lead to simple structures. The biggest disadvantages are variable switching

frequency and the need for high switching frequency to achieve a proper performance. It can be said that switching frequency mostly depends on the amount of selected hysteresis band, sampling frequency, and load parameters. The synchronous reference frame-based method converts the measuring current into active or reactive components and defines reference current values based on active and reactive power. The difference between measuring current and reference current is fed to the PI controllers. Then, these controllers generate voltage reference for the inverter. At the end, the signals are generated for triggering the switches. The disadvantages of this method are: the existence of two PI controllers, the complexity of setting parameters for these two controllers, the necessity of voltage and current fictitious phase for converting the measuring current into active and reactive components of the AC current, and absolute dependence on grid condition. The proportional resonance-controlling method provides the possibility of reaching a steady-state error zero to track the reference signal by providing a very high gain at the fundamental frequency against PI controllers instead of applying the complex synchronous reference frame-based method. Another advantage for this controller is its ability to remove specific harmonics. Among its disadvantages, we can refer to its sensitivity to network frequency changes and current sensor phase-shifting ability [3].

As already mentioned, in most single-phase inverter controls, the fictitious phase is generated for applying the instantaneous power theory. The proper performance of inverter controller is too dependent on generating an accurate fictitious phase which increases the complexity of designing a control system.

In this article, a new method is presented for controlling single-phase grid-connected inverters that does not need to generate a fictitious phase for the current. In this method, the single-phase system is modeled as a three-phase unbalanced system by applying a modified pq theory. In the proposed method, a simple and understandable controlling structure with a quick dynamic response and easy computations has been presented.

This paper is organized as follows: the introduction of pq theory, the proposed method, and the calculation of DC link capacitor are presented in Section II. In Section III, the design of output filter is presented in detail. Comparative simulation and conclusion are expressed in Section IV and V, respectively.

2. SINGLE-PHASE PQ THEORY

In 1983, Professor Akagi introduced the new conceptions of active and reactive instantaneous powers that are valid in steady-state and transition modes for voltage and current waves [23]. The αβ conversion is an algebraic conversion of voltages and currents in a stationary reference frame, also known as Clarke conversion.

Instantaneous power theory is defined for three-phase systems and the conversion of system parameters into two orthogonal axes. Two or more parameters are needed to apply this theory; however, as only one single-phase is available in single-phase systems, this method cannot be directly used. Therefore, a technique is needed to be introduced to solve this problem. The single-phase instantaneous power theory is introduced in reference [24-26]. In this theory, the voltage and current of the network are introduced as α, and fictitious phase β is obtained with a 90-degree shift of network voltage and current. To create this 90-degree shift, different methods such as Hilbert's transformation and second-order generalized integrator (SOGI) are also proposed.

Considering voltage and sinusoidal current, the fictitious phases are obtained as follow:

$$\begin{cases} V_\alpha = V_a = V_m \cos(wt) \\ I_\alpha = I_a = I_m \cos(wt - \varphi) \end{cases} \quad (5)$$

$$\begin{cases} V_\beta = V_m \cos(wt - \frac{\pi}{2}) \\ I_\beta = I_m \cos(wt - \varphi - \frac{\pi}{2}) \end{cases} \quad (6)$$

According to the instantaneous power theory, equations of active and reactive instantaneous power can be expressed as:

$$\begin{cases} p = V_\alpha I_\alpha + V_\beta I_\beta \\ q = -V_\beta I_\alpha + V_\alpha I_\beta \end{cases} \quad (7)$$

Placing Eq. (5) and (6) in (7), the instantaneous active power is

$$\begin{cases} V_\alpha I_\alpha = V_m I_m \cos(wt)\times\cos(wt-\varphi) \\ \qquad = \dfrac{V_m I_m}{2}\left[\cos(2wt-\varphi)+\cos(\varphi)\right] \\ V_\beta I_\beta = V_m I_m \cos(wt-\dfrac{\pi}{2})\times\cos(wt-\varphi-\dfrac{\pi}{2}) \\ \qquad = \dfrac{V_m I_m}{2}\left[\cos(2wt-\varphi-\pi)+\cos(\varphi)\right] \\ p = V_\alpha I_\alpha + V_\beta I_\beta = VI\cos\varphi \end{cases} \quad (8)$$

As can be seen in Eq. (8), creating fictitious phase β and adding in instantaneous power calculation do not change the power value or cause trouble for the system performance. Therefore, it can be said that by generating the fictitious phase, we can benefit from instantaneous power theory in controlling single-phase systems. It is similarly provable for the reactive power.

It is necessary to notice that generating the fictitious phase using methods proposed in references [24-26] requires full recognition of these methods and appropriate adjustments of their parameters. Due to complexities in designing these parameters, system performance is distanced from its proper mode if these tasks, particularly when that they have distortion or harmonics, are not fulfilled properly. In the proposed method, there is no need to generate a fictitious phase for current or use these methods.

2.1. Proposed single-phase pq methods

In this paper, a single-phase system is modeled as a three-phase unbalanced system by applying a modified pq theory for three-phase four-wire systems, such that two fictitious phases, b and c, are created, and their voltage value is the phase voltage with a 120 degree shift, plus zero current. Therefore,

$$\begin{cases} V_a = V_m \sin(wt) \\ V_b = V_m \sin(wt-120) \\ V_c = V_m \sin(wt+120) \end{cases} \quad (9)$$

$$\begin{cases} i_a = I_m \sin(wt+\varphi_I) \\ \mathrm{i}_b = 0 \\ \mathrm{i}_c = 0 \end{cases} \quad (10)$$

The generation of reference currents by the proposed control method is shown simply in Fig. 3.

It is clear that the power extracted from this method is equal to the injected power introduced in Eq. (1). With the proposed method, reference currents can be generated by choosing the power that is supposed to be transferred to the network, without requiring a fictitious phase for current. Based on Fig. 3, a PI controller is also used to control DC link voltage. In the step of controlling the injected power, the output signal of this controller (Pdc) is added to the power which ought to be injected to the network by inverter switching.

2.2. DC link capacitor

As explained in Eq. (4), the instantaneous power injected to the network comprises an average output power and a power variable with time. Because of the performance of maximum power point tracker system (MPPT), the output power of a solar cell ought to be a constant value. Therefore, to balance the power, the pulsating power (P_{grid}-P_{PV}) ought to be controlled by the DC link capacitor. The DC link capacitor is also known as the power decoupling capacitor. Thus, designing and considering a whole number for this capacitor is pivotal for better system performance. Selection of a small value for this capacitor causes an increase in voltage variations at two sides of the capacitor, and troubles the MPPT system performance (ripple in PV module terminal and reduction in average power extracted from PV), and increases distortion in the current injected to the network [27].

Since the pulsating power ought to be controlled by the capacitor, the size of DC link capacitor is obtained as follows [28]:

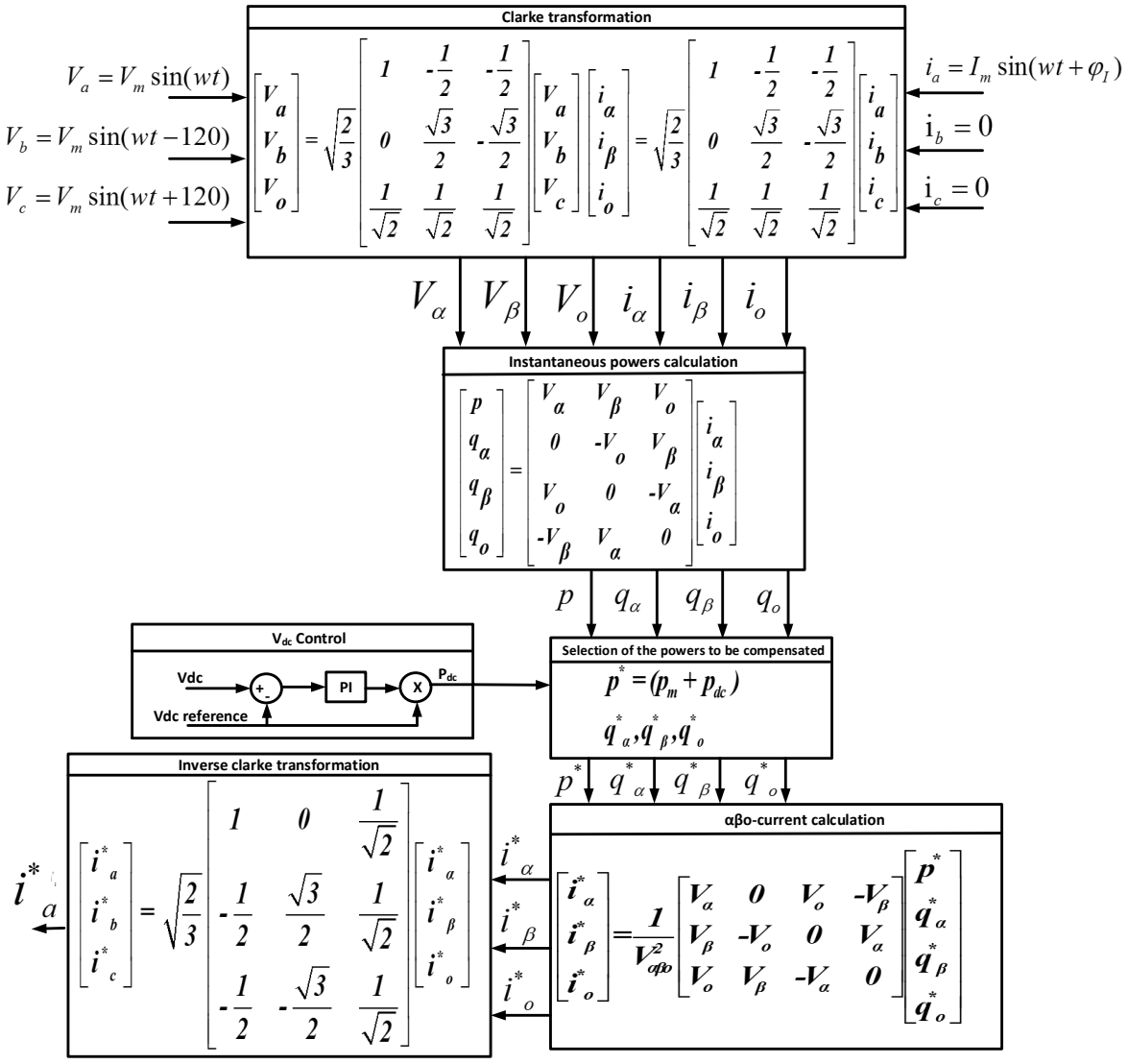

Fig. 3. The proposed control method

$$C = \frac{P_0}{2\pi f V_{dc} \Delta V} \tag{11}$$

where f is grid frequency, V_{dc} is DC link voltage, and ΔV is the allowed value for peak-to-peak voltage variations of DC link.

3. OUTPUT FILTER

To connect the voltage source inverter to the network, a filter is used to reduce harmonics caused by switching. The simplest and most common filter is using an inductor-series. By considering the requisites for inverters' connection and the limited percentage for harmonics, the value for this inductor is selected to be large. The LCL filter is suggested to solve this problem [29-30]. The LCL filter usually has a better damping coefficient. It also remarkably decreases the expenses and size of inductors. Furthermore, the harmonic of switching frequency in the current wave can be reduced by the use of less reactance. The general structure of this filter with the damping resistor is as follows:

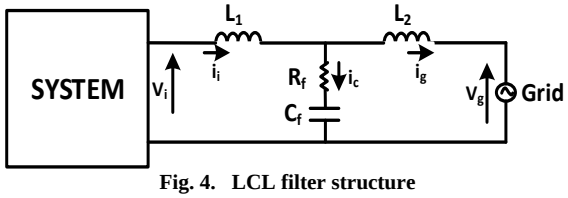

Fig. 4. LCL filter structure

Where, L_1 is the inverter-side inductor and L_2 is the grid-side inductor. C_f and R_f are the damping capacitor and resistor. The required reactive power

may lead to mutual resonance of the capacitor parallel with the network. Therefore, it needs to have a series damping resistor. The extension of the algorithm presented in reference [29] – introduced for a three-phase system – is used in single-phase LCL design. Base impedance and capacitor are calculated as follows:

$$Z_b = \frac{E_n^2}{P_n} \tag{12}$$

$$C_b = \frac{1}{w_g Z_b} \tag{13}$$

Before designing the filter, there are some limitations in design parameters such as:

1) The total amount of inductance (L_1+L_2) must not be more than 10% of the base impedance, otherwise it remarkably drops the voltage and, consequently, requires a higher DC link voltage and increases switching losses.

2) The amount of C_f capacitor is defined by considering maximum variations of the power factor observed by the network whose its value is 5% of the base capacitor. If it is necessary to compensate for the inductive reactance of the filter, higher values can be selected which leads to an increase in system expenses and current ripple.

3) Resonance frequency has to be placed within the following range to avoid resonance problems:

$$10\omega_g < \omega_{res} = \sqrt{\frac{L_1 + L_2}{L_1 L_2 C_f}} < \frac{\omega_{sw}}{2} \tag{14}$$

Steps in designing the filter are expressed as follows:

Step one: Inverter-side inductor calculation

The design of L_1 is the same as the inductive-series filter:

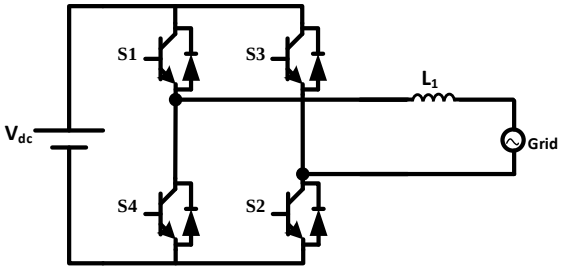

Fig. 5. Inductor-series filter

The output voltage and inductor current variation for the single-phase full-bridge inverter are shown in Figure 6.

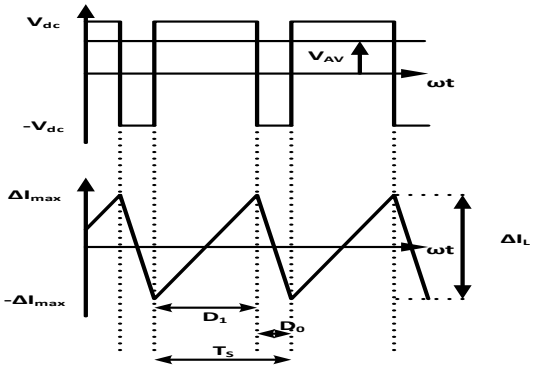

Fig. 6. Output voltage and current waveform of the inductor.

When the switching frequency (f_{sw}) is much higher than the main frequency (50 Hz), it can be said that the average value of the inverter output voltage (V_{av}) in a switching period is a constant value. Therefore, the filter output current or inductor current would be similar to Fig. 7 within every switching period.

The peak-to-peak value for filter output current is obtained as follows:

$$\begin{cases} V_L = L\dfrac{di}{dt} \rightarrow \Delta i_L = \dfrac{1}{L} V_L \Delta t \\ \Delta i_L = 2\Delta i_{L\max} = \dfrac{(V_{dc} - V_{AV})}{L} D_1 T_s \end{cases} \tag{15}$$

According to Fig. 7, the following equations are obtained:

$$\begin{cases} V_{AV}(wt) = \dfrac{1}{T_s}\left(\int_0^{d_1 T_s} V_{dc}\,dt + \int_{d_1 T_s}^{T_s} -V_{dc}\,dt\right) \\ \qquad\qquad = V_{dc}(2D_1(wt) - 1) \\ e_a = m_a V_{dc} \sin(wt) \\ D_1(wt) = \dfrac{1 + m_a \sin(wt)}{2} \end{cases} \tag{16}$$

By placing Equation (16) in Equation (15), the maximum value is calculated for inductor current variation.

$$\Delta i_{L\max} = \frac{\Delta i_{pp}}{2} = \frac{V_{dc} T_s}{4L}(1 - m_a^2 \sin^2(wt)) \quad (17)$$

The maximum value for inductor current variations is:

$$\Delta i_{L\max} = \frac{V_{dc} T_s}{4L} \quad (18)$$

Thus, by selecting $\Delta i_{L\max} = (10\% - 20\%) I_{pp}$ where I_{pp} is the peak-to-peak value for the output current, the inductor value of the inverter-side is obtained.

$$L_1 = \frac{V_{dc} T_s}{4\Delta i_{L\max}} \quad (19)$$

Step two: Calculation of parallel branch capacitor

As previously mentioned, the value of capacitor is 5% of the base capacitor.

$$C_f = 0.05 C_b \quad (20)$$

Step three: Calculation of grid-side inductor

With the definition of attenuation coefficient (k_a) that shows the proportion of harmonic current produced by the inverter and the current injected to the grid, the equation for L_2 calculation can be obtained [29]:

$$\frac{i_g(\mathrm{h})}{i_i(\mathrm{h})} = k_a \quad (21)$$

$$L_2 = \frac{\sqrt{\frac{1}{k_a^2} + 1}}{C_f w_{sw}^2} \quad (22)$$

where k_a is the attenuation coefficient, C_f is the parallel-branch capacitor, and ω_{sw} is the switching frequency. To have the least resonance, the L_2 value can be chosen equal to L_1; nevertheless, reference [29] demonstrates that a smaller value for L_2 can be selected without any problems in the system by choosing a lower attenuation coefficient. It is necessary to notice that as the inductor size at the side of grid increases, higher expenses are imposed on the system.

Step four: Investigation of pre-design conditions

In case of pre-design conditions, if resonance frequency range and the whole filter impedance are not met, we go back to Step three and change the attenuation coefficient.

Step five: Calculation of damping resistance

In order to improve damping resonance, the resistor size is set to $\frac{1}{3}$ of the series capacitor impedance. If the value for this resistor is selected to be large, system losses are increased and the overall efficiency is reduced.

$$R_f = \frac{1}{3 w_{res} C_f} \quad (23)$$

4. ANALYSIS AND SIMULATION RESULTS

Figure 7 shows the general structure of the control system of single-phase inverter connected to the grid. The controlling signal for DC/DC converter is produced by measuring the voltage and current of PV module and also by applying the perturb and observe (P&O) method for MPPT system. As mentioned earlier, a PI controller is used to reduce error deviation -caused by DC link voltage and voltage reference- .The inverter controller is picked from the structures explained in Fig. 3. The accuracy of the proposed controlling method was assessed by Matlab/Simulink and the sampling time was 1 μs.

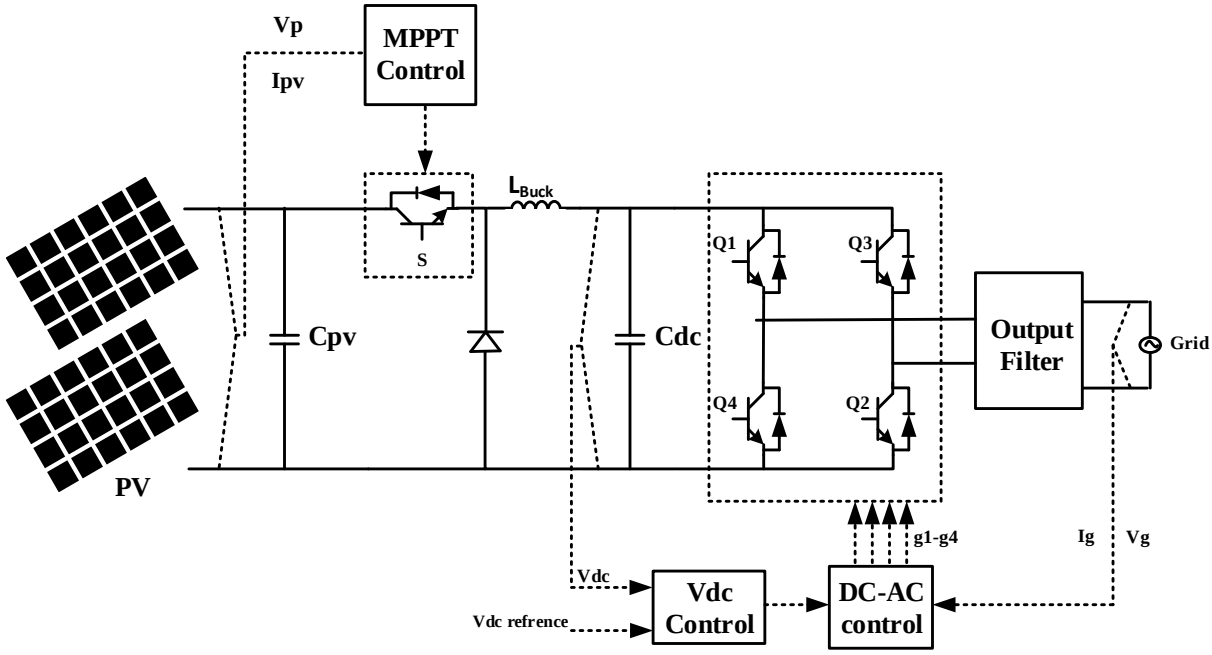

Fig. 7. Structure of the inverter control system.

To verify the proposed method, simulation results were compared with the results of the conventional current hysteresis control (CHC) technique [8]. The average switching frequency is used due to the variable switching frequency in the hysteresis method and for a better comparison of the result of the proposed method. The average switching frequency fh is defined as fh=Nh/T, where Nh is the number of switching operations for one switch of inverter and T is the simulation time. To simulate the PV module, information from the 3Kw photovoltaic system installed at Birjand University is used. This information is summarized in Table 1. and general parameters of the system are mentioned in Table 2.

As the PV module voltage is higher than the level of single-phase system voltage at its maximum power point, a Buck converter is used to reduce DC link voltage for connecting the inverter to the single-phase grid. The LCL filter has been designed according to Section (3) and its parameter values are listed in Table 2.As the PV module voltage is higher than the level of single-phase system voltage at its maximum power point, a Buck converter is used to reduce DC link voltage for connecting the inverter to the single-phase grid. The LCL filter has been designed according to Section (3) and its parameter values are listed in Table 2.

Table 1. Photovoltaic system parameter

Symbol	Parameter	Value
I_{Sc}	Short circuit current	8.21
K_I	Temperature coefficient of Isc	0.0032
V_{oc}	Open circuit voltage	32.9
K_V	Temperature coefficient of Voc	-0.123
N_S	Cells per module	54
N_{SS}	Series-connected modules per string	15
N_P	Parallel cells	1
N_{PP}	Parallel modules	1
R_S	Series resistance	0.23
R_t	Shunt resistance	601.3368
V_{mp}	Voltage at maximum power point	26.3
I_{mp}	Current at maximum power point	7.61
P	Maximum Power	kW 3

Figure 8 compares the DC link voltage and ripple of DC link voltage of the proposed method and CHC whose reference value is set to $2\sqrt{220}$. The value for this oscillation (ripple) is equal to the value which was placed in DC link capacitor calculation for variations of DC link voltage in Eq. (11). As described in this equation, if less oscillations are intended, we only needed to choose a smaller value for ΔV that increases the DC link capacitance. Figures 8 and 9 show that the proposed method has a good

convergence speed in comparison with hysteresis to the desired value of DC link voltage.

The current injected to the grid is presented in Fig. 9. It can be noted that both can transfer the PV module power to the grid with a small harmonic value.

The harmonic spectrum of the injected current is shown in Fig. 10, where THD is less than %5. As can be seen, there are a few harmonics at the switching frequency. However, this amount of harmonics meets the requisites and standards in connecting to the grid. Meanwhile, THD can be reduced with increasing the inductor size at the inverter-side or switching frequency. Nevertheless, it increase the costs. According to Figure 10, the current harmonics in CHC are mostly at sampling frequency multiplied by average switching frequency. In the CHC method, a proper performance is obtained by choosing a narrow bandwidth and high average switching frequency that leads to the increase of switching losses and system costs. The quality of the proposed method is comparable to that of the CHC method with a high average switching frequency.

Table 2. Test system parameter

Symbol	Parameter	Value
f_g	Grid frequency	50 Hz
f_{sw}	Switching frequency	KHz 10
V_{grid}	rms grid voltage	220 V
L_1	Inverter-side inductor	2 mH
L_2	Grid-side inductor	150 µH
C_f	Capacitor of filter	10 µF
R_f	Damping resistance	1.25 Ω
C_{dc}	DC link capacitor	3.9 mF
L	Inductor of buck converter	0.5 mH
C_{pv}	Input capacitor of PV	100 µF
K_p	The proportional gain of DC link voltage controller	0.01
K_i	The integral gain of DC link voltage controller	4.1

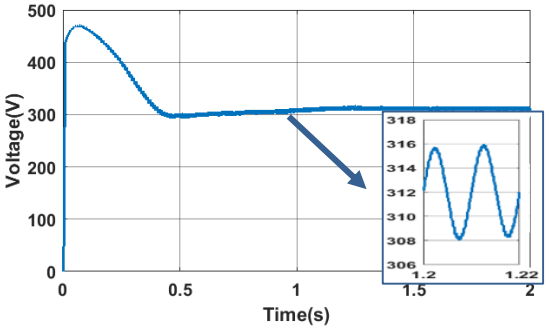

(a)

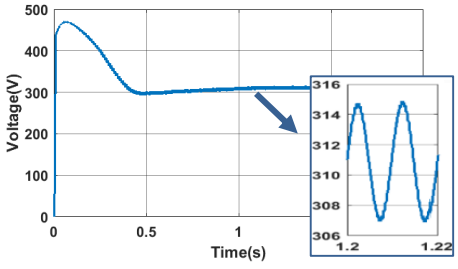

(b)

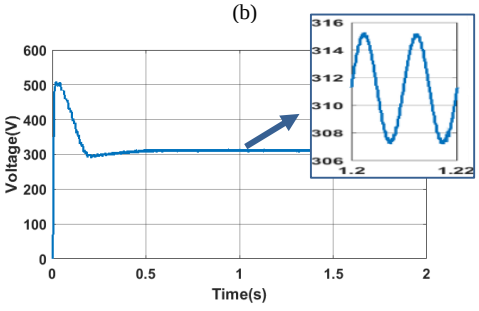

(c)

Fig. 8. DC link voltage (a) CHC (10 kHz) (b).CHC (20 kHz) (c) Proposed method

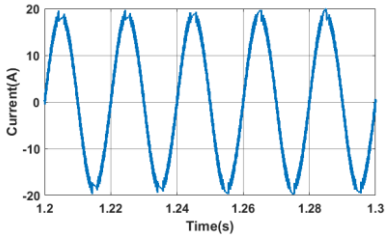

(a)

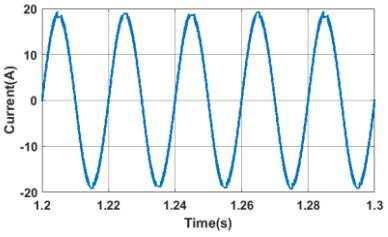

(b)

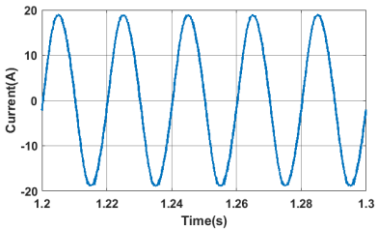

(c)

Fig. 9. Injected current to grid (a) CHC (10 kHz) (b) CHC (20 kHz) (c) Proposed method

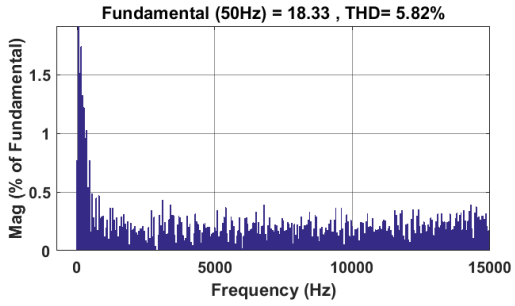

(a)

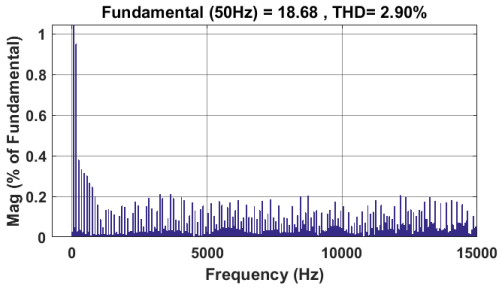

(b)

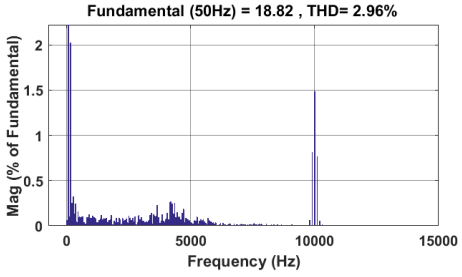

(c)

Fig. 10. Injected current harmonic spectrum (a) CHC (10 kHz) (b) CHC (20 kHz) (c) Proposed method

The sinusoidal injected current with low THD and the DC link voltage converging on the desired amount confirm that the proposed method can successfully have a proper performance. Furthermore, as can be seen in Fig. 9 and 10, the output current of the inverter is smooth and the harmonic examination shows the effectiveness of the designed filter. The amount of instantaneous power injected to the network is presented in Fig. 11. As described in Eq. (4), the amount of average output power is fairly equal to the PV module power.

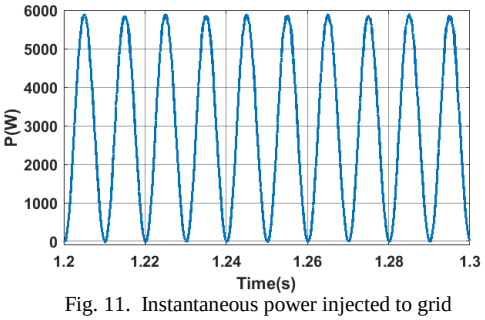

Fig. 11. Instantaneous power injected to grid

Voltage, current, and PV module power are shown in Fig. 12. The proposed controlling method does not have an undesirable performance over the power point tracking system, and the output properties of PV with small ripple value are fixed on the conditions of the highest output power.

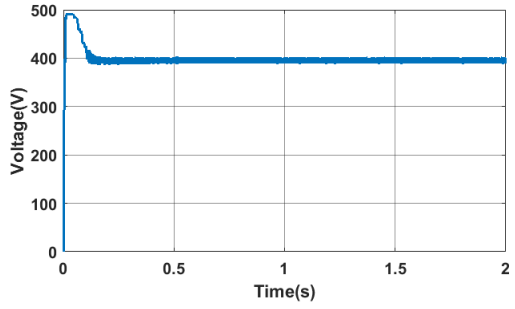

(a)

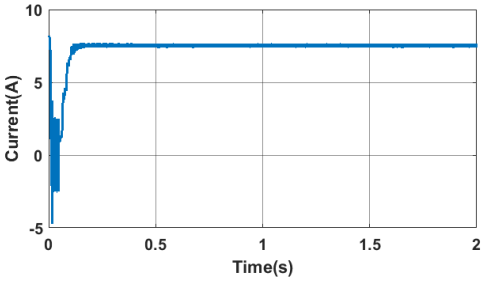

(b)

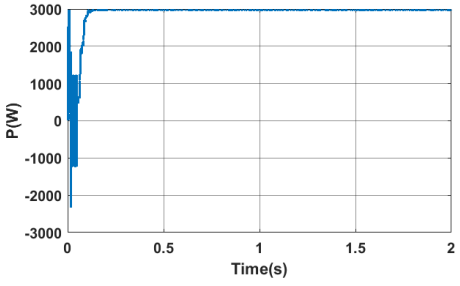

(c)

Fig. 12. PV module (a).Voltage (b).Current (c).Power

5. CONCLUSION

In this paper, a new current control strategy based on single-phase pq theory is proposed for single-phase grid-connected LCL-filtered VSI. In the proposed technique, the reference currents are generated by applying a modified pq theory. The comparative simulation results confirm that the by modeling a single-phase system as a three-phase imbalanced system with two phase currents of zero, the inverter has a good performance and fast response without the current and power injected to the network being removed out of their desirable state. Furthermore, without fictitious current phase generation, the simplicity of the controlling system is increased. Finally, the simulation results show that the proposed control method achieves the required control objectives such as fast response, proper performance of power point tracking system, low ripple of DC link voltage, instantaneous power balance and sinusoidal grid current with low THD.

REFERENCES

[1] M. Schmela,"Global market outlook for solar power/2016-2020" , EPIA, Belgium, 2016.

[2] H. Komurcugil, N. Altin, S. Ozdemir and I. Sefa "Lyapunov-function and proportional-resonant-based control strategy for single-phase grid-connected VSI with LCL filter," *IEEE Trans. Ind. Electron.*, vol. 63, no. 5, pp. 2838-2849, 2016.

[3] M. Monfared and S. Golestan "Control strategies for single-phase grid integration of small-scale renewable energy sources: A review," *Renewable Sustainable Energy Rev.*, vol. 16, pp. 4982-4993, 2012.

[4] Y. Shi, B. Liu and S. Duan "Low-frequency input current ripple reduction based on load current feedforward in a two-stage single-phase inverter," *IEEE Trans. Power Electron.*, vol. 31, no. 11, pp. 7972-7985, 2016.

[5] Y. Hu, Y. Du, W. Xiao, S. Finney and W. Cao "DC-link voltage control strategy for reducing capacitance and total harmonic distortion in single-phase grid-connected photovoltaic inverters," *IET Power Electron.*, vol. 8, no. 8, pp. 1386-1393, 2015.

[6] G. Zhu, X. Ruan, L. Zhang and X. Wang "On the reduction of second harmonic current and improvement of dynamic response for two-stage single-phase inverter," *IEEE Trans. Power Electron.*, vol. 30, no. 2, pp. 1028-1041, 2015.

[7] M. Banaei "Multi-stage DC-AC converter based on new DC-DC converter for energy conversion," *J. Oper. Autom. Power Eng.*, vol. 4, no. 1, pp. 42-53, 2016.

[8] M. Kumar; R. Gupta "Sampled-Time Domain Analysis of Digitally Implemented Current Controlled Inverter," *IEEE Trans. Ind. Electron.*, vol. PP, no.99, pp.1-1, 2016

[9] F. Wu, F. Feng, L. Luo J. Duan and L. Sun "Sampling period online adjusting-based hysteresis current control without band with constant switching frequency," *IEEE Trans. Ind. Electron.*, vol. 62, no. 1, pp. 270-277, 2015.

[10] S. Gautam and R. Gupta "Unified time-domain formulation of switching frequency for hysteresis current controlled AC/DC and DC/AC grid connected converters," *IET Power Electron.*, vol. 6, pp. 683-692, 2013.

[11] Z. Yao and L. Xiao "Control of single-phase grid-connected inverters with nonlinear loads," *IEEE Trans. Ind. Electron.*, vol. 60, pp. 1384-138, 2013.

[12] F. Wu, L. Zhang, and Q. Wu "Simple unipolar maximum switching frequency limited hysteresis current control for grid-connected inverter," *IET Power Electron.*, vol. 7, pp. 933-945, 2014.

[13] M. Ebrahimi, S. A. Khajehoddin and M. Karimi-Ghartemani "Fast and robust single-phase DQ current controller for smart inverter applications," *IEEE Trans. Power Electron.*, vol. 31, no. 5, pp. 3968-3976, 2016.

[14] S. Somkun and V. Chunkag "Unified unbalanced synchronous reference frame current control for single-phase grid-connected voltage-source converters," *IEEE Trans. Ind. Electron.*, vol. 63, no. 9, pp. 5425-5436, 2016.

[15] Shuhui Li, Xingang Fu, Malek Ramezani, Yang Sun, Hoyun Won "A novel direct-current vector control technique for single-phase inverter with L, LC and LCL filters," *Electr. Power Syst. Res.*, vol. 125, pp. 235-244, 2015

[16] B. Bahrani, M. Vasiladiotis, and A. Rufer "High-order vector control of grid-connected voltage-source converters with LCL-filters," *IEEE Trans. Ind. Electron.*, vol. 61, pp. 2767-2775, 2014.

[17] M. Monfared, S. Golestan, and J. M. Guerrero "Analysis, design, and experimental verification of a synchronous reference frame voltage control for single-phase inverters," *IEEE Trans. Ind. Electron.*, vol. 61, pp. 258-269, 2014.

[18] T. Ye, N. Dai, C. S. Lam, M. C. Wong and J. M. Guerrero "Analysis, design, and implementation of a quasi-proportional-resonant controller for a multifunctional capacitive-coupling grid-connected inverter," *IEEE Trans. Ind. Appl.*, vol. 52, no. 5, pp. 4269-4280, 2016.

[19] G. Shen, X. Zhu, J. Zhang and D. Xu "A new feedback method for PR current control of LCL-filter-based grid-connected inverter," *IEEE Trans. Ind. Electron.*, vol. 57, no. 6, pp. 2033-2041,2010.

[20] M. Castilla, J. Miret, J. Matas, L. G. d. Vicuna, and J. M. Guerrero "Linear current control scheme with series resonant harmonic compensator for single-phase grid-connected photovoltaic inverters," *IEEE Trans. Ind. Electron.*, vol. 55, pp. 2724-2733, 2008.

[21] M. Castilla, J. Miret, J. Matas, L. G. d. Vicuna, and J. M. Guerrero "Control design guidelines for single-phase grid-connected photovoltaic inverters with damped resonant harmonic compensators," *IEEE Trans. Ind. Electron.*, vol. 56, pp. 4492-4501, 2009.

[22] J. He and Y. W. Li "Hybrid voltage and current control approach for DG-grid interfacing converters with LCL filters," *IEEE Trans. Ind. Electron.*, vol. 60, pp. 1797-1809, 2013.

[23] H. Akagi, E. H. Watanabe, M. Aredes, Instantaneous power theory and applications to power conditioning, Wiley-IEEE Press, 2007, pp. 41-107.

[24] W. Song, Z. Deng, S. Wang and X. Feng "A simple model predictive power control strategy for single-phase PWM converters with modulation function optimization," *IEEE Trans. Power Electron.*, vol. 31, no. 7, pp. 5279-5289, 2016.

[25] V. Khadkikar and A. Chandra "A novel structure for three-phase four-wire distribution system utilizing unified power quality conditioner (UPQC)," *IEEE Trans. Ind. Appl.*, vol. 45, no. 5, pp. 1897-1902, 2009.

[26] R. I. Bojoi, L. R. Limongi, D. Roiu and A. Tenconi "Enhanced power quality control strategy for single-phase inverters in distributed generation systems," *IEEE Trans. Power Electron.*, vol. 26, no. 3, pp. 798-806, 2011.

[27] X. Zong, A single phase grid connected DC/AC inverter with reactive power control for residential PV application, M.S. Thesis, Dept. Elec. Eng., Toronto Univ., Toronto, 2011.

[28] P. T. Krein, R. S. Balog, and M. Mirjafari "Minimum energy and capacitance requirements for single-phase inverters and rectifiers using a ripple port," *IEEE Trans. Power Electron.* vol. 27, pp. 4690-4698, 2012.

[29] A. Reznik, M. G. Sim, A. Al-Durra, and S. M. Muyeen "Filter design and performance analysis for grid-interconnected systems," *IEEE Trans. Ind. Appl.*, vol. 50, pp. 1225-1232, 2014.

[30] M. Farhadi Kangarlu, E. Babaei, F. Blaabjerg "An LCL-filtered single-phase multilevel inverter for grid integration of PV systems," *J. Oper. Autom. Power Eng.*, vol. 4, no. 1, pp. 54-65, 2016.